Mid-infrared spectra of the proton-bound complexes Ne_n–HCO^+ (n=1,2)

Sergey A. Nizkorodov, Otto Dopfer,[a] Markus Meuwly, John P. Maier, and Evan J. Bieske[b]
Institut für Physikalische Chemie, Universität Basel, Klingelbergstrasse 80, CH-4056 Basel, Switzerland

(Received 6 February 1996; accepted 24 April 1996)

The ν_1 band of Ne–HCO^+ has been recorded for both ^{20}Ne and ^{22}Ne containing isotopomers by means of infrared photodissociation spectroscopy. The rotational structure of the band is consistent with a parallel Σ–Σ type transition of a linear proton-bound complex. The following constants are extracted for ^{20}Ne–HCO^+: ν_0=3046.120±0.006 cm^{-1}, B''=0.099 54±0.000 05 cm^{-1}, $D''=(5.30\pm0.30)\times10^{-7}$ cm^{-1}, $H''=(1.1\pm0.9)\times10^{-11}$ cm^{-1}, B'=0.100 03±0.000 05 cm^{-1}, $D'=(4.89\pm0.30)\times10^{-7}$ cm^{-1}, $H'=(1.6\pm0.9)\times10^{-11}$ cm^{-1}. The ν_1 band is redshifted by 42.5 cm^{-1} from the corresponding ν_1 transition of free HCO^+ indicating that the Ne atom has a pronounced influence on the proton motion. Linewidths for individual rovibrational transitions are laser bandwidth limited, demonstrating that the lifetime of the ν_1 level is at least 250 ps. An approximate radial potential for the collinear Ne$\cdots HCO^+$ interaction is constructed by joining the mid-range potential obtained from a Rydberg–Klein–Rees inversion of the spectroscopic data to the theoretical long-range polarization potential. Based on this potential, the estimated dissociation energy (D_0) for Ne–HCO^+ is 438 cm^{-1} in the (000) state and 454 cm^{-1} in the (100) excited state. The rotationally unresolved ν_1 band of $^{20}Ne_2$–HCO^+ is slightly blueshifted with respect to that of ^{20}Ne–HCO^+. The observed frequency shift is compatible with a trimer structure where the second Ne atom is attached to the linear Ne–HCO^+ dimer core. © *1996 American Institute of Physics.* [S0021-9606(96)01129-4]

I. INTRODUCTION

During the past few years there have been an increasing number of studies devoted to the spectroscopy and dynamics of small ionic complexes, often undertaken with the goal of furnishing information on the mid-range interaction between ions and neutrals. The development of sensitive and selective experimental techniques has recently led to rapid improvement in the quality of spectroscopic data, with rotationally resolved spectra having been obtained for several smaller systems.[1,2] In our laboratory the focus has been on simple proton-bound cation dimers, systems where two bases are bound through an intermediate proton. Mid-infrared, rotationally resolved studies of complexes such as He–HN_2^+,[3,4] He–HCO^+,[5] Ar–HCO^+,[6] and H_2–HCO^+ (Ref. 7) have yielded information on structures and intermolecular bond strengths. Whereas in some regards the structure and dynamics of ionic complexes like Ne–HCO^+ are similar to the ones of the isoelectronic neutrals (e.g., Ne–HCN),[8] with both ions and neutrals possessing a linear equilibrium geometry, generally the ionic systems are somewhat more strongly bound and feature a much less labile intermolecular bond.

There are several reasons why the Rg–HCO^+ series (Rg =rare gas) is useful for exploring the sharing of a proton between two Lewis bases. In the first place the HCO^+ cation, which functions as the chromophore of the Rg–HCO^+ complexes, is one of the better characterized polyatomic molecular ions, having been comprehensively studied in the infrared (ν_1=3089 cm^{-1},[9,10] ν_2=828 cm^{-1},[11,12] ν_3=2184 cm^{-1} [13]) and microwave[14,15] spectral regions as well as in several theoretical studies.[16] It is known to be linear, having a $^1\Sigma^+$ symmetry ground electronic state, and possesses no low-lying excited electronic states.[16] Second, while the systems are sufficiently simple to yield spectra that are understandable within the compass of established spectroscopic paradigms, they display essential features of more complicated proton-transfer contexts, and so may serve as launching pads for a better understanding of proton transfer in biological and organic systems.

Characterization of complexes like Ne–HCO^+ is also relevant because of their role as intermediates in gas phase protonation reactions (e.g., $NeH^+ + CO \rightarrow HCO^+ + Ne$). Although flow tube studies have yielded rates for exothermic proton transfer reactions,[17] the precise details of both the energy partitioning among the product vibrational and rotational degrees of freedom and the influence of reactant excitation on the reaction rate remain obscure. A more comprehensive understanding of the reaction intermediates' potential energy surface may help to clarify these issues.

A particular objective of the current mid-infrared study of Ne–HCO^+ is to furnish data that will enable a systematic exploration of the effect of changing one base (He, Ne, Ar, H_2) in a proton-bound complex while the other (CO) remains the same. The relatively high proton affinity of CO (141.5 kcal/mol) compared to that of He, Ne, Ar, and H_2 (42.5, 48.1, 88.6, and 101 kcal/mol, respectively)[18] means that all of the complexes can be approximately considered to consist of a HCO^+ core loosely attached to the other ligand. However, due to marginal proton transfer, the core properties are slightly modified with a flattening of the effective proton

[a]Author to whom correspondence should be addressed.
[b]Present address: School of Chemistry, The University of Melbourne, Parkville, Victoria 3052, Australia.

 0021-9606/96/105(5)/1770/8/$10.00

potential and a consequent redshift of the HCO^+ ν_1 vibration (C–H stretch).

While the IR spectroscopic data provide a convenient impression of the interaction between the Ne atom and the HCO^+ molecule near the potential minimum, other properties of the complex such as the dissociation energy and frequencies of the higher intermolecular stretching levels, require a potential out to the dissociation limit. In the present study such a radial potential is generated by using spectroscopic data to construct a RKR potential in the potential minimum region, while the long-range part of the potential is assumed to have the form consistent with the polarization interaction between the Ne atom and the HCO^+ molecular ion.

The experiments with the Ne_1–HCO^+ and Ne_2–HCO^+ continue efforts toward eludicating the microsolvation of molecular ions by rare gas atoms. Recently, the solvation of a HCO^+ ion by Ar has been explored[6] by following the development with increasing Ar_n–HCO^+ cluster size of a number of cluster properties including the C–H stretch vibrational frequency, frequencies for combination bands involving the intermolecular stretch vibration, vibrational band shapes, and Ar atom binding energies (derived from fragmentation branching ratios). In conjunction with simple empirical model calculations, the experimental data suggest cluster geometries in which the first Ar atom occupies a privileged linear proton-bound configuration, while additional Ar atoms fill primary and secondary solvation rings around the linear Ar–HCO^+ core (each ring containing up to five Ar atoms). The first solvation shell is completed at Ar_{12}–HCO^+, which possesses an icosahedral-type structure. Unfortunately, efforts to follow a similar course for He and Ne containing complexes have been frustrated by lower ion currents for clusters containing more than two rare gas atoms. However, on the basis of the ν_1 vibrational band shifts, it appears that the He_2–HN_2^+ trimer (like Ar_2–HCO^+) has a structure in which one rare gas atom is situated in a linear proton-bound configuration with the second more loosely attached.[4,6]

II. EXPERIMENT

The spectroscopic characterization of weakly bound ionic species using traditional techniques is often hampered by problems of selectivity and sensitivity. One must not only generate sufficient densities of the desired ionic cluster, but must also decide which spectral features are due to which ionic (or neutral) molecular species in what is inevitably a complex chemical environment. A convenient way of circumventing these problems is to undertake investigations in a tandem mass spectrometer, confining attention to weakly bound species that fragment following photoexcitation. For such complexes a spectrum can be obtained by scanning the wavelength of the light source while monitoring the intensity of the fragment ion peak. Mass selection of parent and fragment ions ensures (in most cases) unambiguous identification of the photoactive species. Single fragment ion detection efficiencies guarantee exceptionally high sensitivities. It is by this approach that ν_1 spectra of Ne_n–HCO^+ ($n=1,2$) have been recorded.

The experimental setup is in essence a tandem mass spectrometer coupled with an electron-impact ion source. The mass spectrometer comprises a primary quadrupole mass filter for initial ion selection, an octopole ion guide where the parent ion beam is overlapped with the output of a pulsed tunable IR radiation source, and a second quadrupole mass filter tuned to the mass of the daughter ions. Eventually, the fragment ions are sensed with a Daly detector[19] connected to a gated boxcar integrator. Complete details of the experimental procedure have been outlined in previous publications dealing with IR vibrational predissociation spectroscopy of proton-bound complexes[6,7] and in a recent review.[20]

The Ne_n–HCO^+ complexes were synthesized from a mixture of Ne, H_2, and CO (ratio 400:20:1) at 4 bar stagnation pressure in a pulsed and skimmed supersonic expansion crossed by electron beams originating from two filaments close to the nozzle orifice. Initial optimization of the Ne_n–HCO^+ ion signal was accomplished by introducing buffer gas (He or N_2) into the octopole region with the second quadrupole tuned to the Ne_{n-1}–HCO^+ collision-induced dissociation product. Subsequently, the laser-induced fragmentation signal was maximized by tuning the laser to a cluster resonance. The parent cluster ion signal was sensitive to the position of the nozzle with respect to the electron emitting filaments and also to the composition of the gas mixture (optimized with a computer-controlled on-line gas mixer), both observations are signs of a weakly bound complex. As expected, under typical conditions the ion current issuing from the ion source is dominated by the HCO^+ molecular ion, with the Ne_n–HCO^+ current being several orders of magnitude smaller. Although the isomeric HOC^+ form (isoformyl cation) is also known to exist, it is less stable and has been shown to convert rapidly to HCO^+ through collisions with either H_2 or CO.[21–23] Given the substantial fraction of both H_2 and CO in the expanding gas mixture, more or less complete conversion from HOC^+ to HCO^+ can be anticipated. Preliminary IR spectral searches were thus concentrated in the region of the strong HCO^+ ν_1 band near 3.2 μm.

Pulsed tunable infrared light (3.5 ns) is generated using a Nd:YAG pumped optical parametric oscillator system which simultaneously produces light in the 1.6 and 3.2 μm ranges (near- and mid-infrared output, respectively) with a bandwidth of less than 0.02 cm^{-1}. The Ne_n–HCO^+ spectra were calibrated against known absorptions of OCS (mid-infrared output) and HDO (near-infrared output),[24] with accurate interpolation between the measured optoacoustic lines facilitated by simultaneously recording etalon fringes. Ions pass through the octopole ion guide with 6.0 ± 0.5 eV of translational energy necessitating a small positive Doppler correction ($\sim$0.05 cm^{-1}) to the measured line wave numbers and providing a small contribution ($\sim$0.005 cm^{-1}) to the Ne–HCO^+ rovibrational linewidths. To compensate for any drifts in the background signal (e.g., metastable and

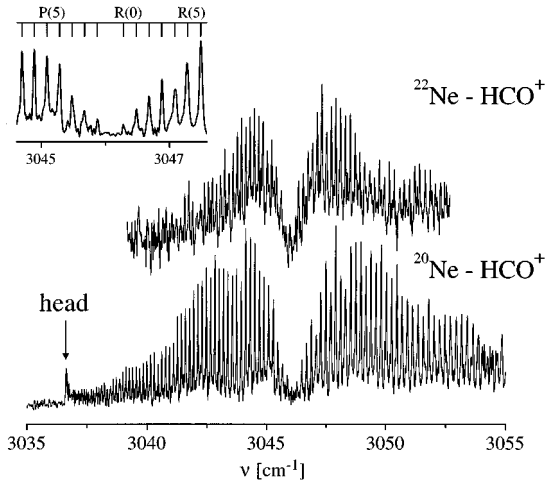

FIG. 1. Vibrational predissociation spectra of ^{20}Ne–HCO^+ and ^{22}Ne–HCO^+ (high-power scan) taken in the vicinity of the C–H stretch band (ν_1) by monitoring the HCO^+ photofragment signal as a function of IR frequency. The inset shows the ^{20}Ne–HCO^+ spectrum near the $4B$ band gap.

collision-induced fragmentation) the nozzle was triggered at twice the laser frequency (20 Hz), with the laser-off signal being subtracted from the laser-on signal.

III. RESULTS AND DISCUSSION

A. Ne–HCO$^+$

1. Mid-IR spectra

Scans in the 2960–3390 cm^{-1} range revealed a prominent Σ–Σ transition centered near 3046 cm^{-1} for both ^{20}Ne–HCO^+ and ^{22}Ne–HCO^+ which is assigned to the ν_1 vibration (C–H stretch) of the respective complexes (see Fig. 1). The ^{20}Ne–HCO^+ spectrum was recorded with reduced laser power (50 μJ/pulse) displaying a flat background and laser limited linewidths implying a lower value for the upper state lifetime of 250 ps. For the less abundant isomer, the higher laser power (0.5–1.0 mJ/pulse) necessary to obtain spectra with reasonable signal-to-noise ratio, leads to rotational line broadening and to the appearance of a background underlying the P and R branches. Additional weaker structure, shifted slightly to the blue of the main peak and extending up to 3100 cm^{-1} (not shown in Fig. 1), is apparent in the ^{20}Ne–HCO^+ spectrum and is almost certainly due to combination bands of intermolecular modes with ν_1 and/or sequence bands involving ν_1 and intermolecular vibrations.

Whereas for ^{20}Ne–HCO^+ the $P(1)$ and $R(0)$ lines are clearly apparent and rotational numbering is straightforward (see the inset of Fig. 1), for ^{22}Ne–HCO^+ a poorer signal-to-noise ratio makes numbering more difficult. However, examination of the band-gap region in several independent spectra prompted a numbering whereby the origin of the ^{22}Ne–HCO^+ transition lies 0.106 cm^{-1} below the one of ^{20}Ne–HCO^+. The following transitions have been observed and assigned: $P(1)$–$P(61)$ and $R(0)$–$R(51)$ for ^{20}Ne–HCO^+, and $P(1)$–$P(25)$ and $R(0)$–$R(30)$ in the case of ^{22}Ne–HCO^+. A least-squares fit of the transition energies to the pseudodiatomic expression

$$\begin{aligned}\nu_{\rm obs} = \nu_0 &+ B'[J'(J'+1)] - D'[J'(J'+1)]^2 \\ &+ H'[J'(J'+1)]^3 - B''[J''(J''+1)] \\ &+ D''[J''(J''+1)]^2 - H''[J''(J''+1)]^3 \end{aligned} \quad (1)$$

yields the parameters presented in Table I. The quality of the fit is evident from the relatively low standard deviation (0.003 and 0.006 for $^{20/22}Ne$–HCO^+, respectively). Ground and excited state B, D, and H values obtained by forming the appropriate combination differences did not differ within the error margins from the ones given in Table I. While for ^{22}Ne–HCO^+ the rotational line positions were fit within experimental error using only B and D values, for ^{20}Ne–HCO^+ the quality of the fit was slightly improved by including H values, although their uncertainties are of the same order as the values themselves. The head in the P branch (at $J'' \approx 70$) is the result of the slightly larger B value in the upper state.

The uncomplicated nature of the Ne–HCO^+ ν_1 spectrum, consisting of a single strong band with regular P and R branches, a $4B$ band gap, and the absence of a Q branch, suggests that the complex has a linear equilibrium structure. Assuming that the ν_1 transition moment remains directed

TABLE I. Constants (in cm^{-1}) for the ground (000) and ν_1 (100) levels of the ^{20}Ne–HCO^+ and ^{22}Ne–HCO^+ isotopomers obtained from the fit of experimental line positions to the linear pseudodiatomic Hamiltonian [Eq. (1)]. Center-of-mass distances (in Å) of the intermolecular bond are evaluated from the rotational constants assuming an undistorted HCO^+ monomer [Eq. (2)]. The harmonic stretching frequencies ν_s (in cm^{-1}) and the force constants k_s (in N/m) are also included [Eqs. (3) and (4)]. Uncertainties in the centrifugal distortion constants carry over into the corresponding ν_s values. Uncertainties (2σ) in the last two digits of the constants follow each value in parenthesis.

	^{20}Ne–HCO^+ (000)	^{20}Ne–HCO^+ (100)	^{22}Ne–HCO^+ (000)	^{22}Ne–HCO^+ (100)
ν_0		3046.120 (06)		3046.014 (06)
B	0.099 54 (05)	0.100 03 (05)	0.094 50 (15)	0.094 99 (15)
$D(\times 10^{-7})$	5.30 (30)	4.89 (30)	3.4 (1.8)	3.1 (1.5)
$H(\times 10^{-11})$	1.1 (9)	1.6 (9)		
$r_{\rm c.m.}$(Ne–HCO^+)	3.654 (01)	3.643 (01)	3.655 (03)	3.644 (03)
ν_s	83.3 (2.5)	87.4 (3.0)		
k_s	4.84 (30)	5.32 (36)		

along the HCO^+ axis, a rigid nonlinear structure would result in the appearance of a Q branch and more complicated patterns in the P and R branches. On the other hand, a free internal rotor structure, where there is little impedance to the internal rotation of the HCO^+, would lead to the occurrence of more widely spaced bands associated with ± 1 changes in the internal rotation quantum number j, again contrary to observation.

Assuming that the HCO^+ monomer is not distorted by the presence of the Ne atom and neglecting zero-point-energy effects, an approximate separation between the center-of-mass of the monomer and the Ne atom can be estimated from the formula[25]

$$r_{\text{c.m.}} = \sqrt{F(1/B_{\text{complex}} - 1/B_{\text{HCO}^+})/\mu_{\text{complex}}}, \tag{2}$$

where $F = 16.857\,63$ is the conversion factor between the moment of inertia (in amu Å^2) and the rotational constant (in cm^{-1}), and μ_{complex} is the reduced mass of the complex. For ^{20}Ne–HCO^+ this gives values of 3.654 Å for the ground state and 3.643 Å for the ν_1 vibrational state, respectively, i.e., the intermolecular bond length decreases by 0.011 Å upon ν_1 excitation (Table I). In principle, the Ne atom can approach the HCO^+ core from either the oxygen or the hydrogen end to form a linear complex. With the ground state HCO^+ substitution structure taken from Woods[15] Ne–O and Ne–H distances can be estimated as 3.12 Å for the Ne–OCH^+ and 1.99 Å for the Ne–HCO^+ structures, respectively. One can almost certainly rule out the oxygen-bonded structure on the basis of the substantial ν_1 (C–H stretch) vibrational band shift (-42.5 cm^{-1}), which is more consistent with a geometry where the proton is adjacent to the Ne atom. This is in line with observations for neutral hydrogen-bonded complexes. For example, in the linear van der Waals dimer HCN–HF, the free C–H stretching frequency is practically unaffected by complex formation, whereas the bonded hydrogen stretch (F–H stretch) frequency is reduced by around 245 cm^{-1}.[26] A proton-bound Ne–HCO^+ structure is also consistent with *ab initio* calculations and experimental findings on similar species including H_2–HCO^+,[7,22,27] He–HCO^+,[5] H_2–HN_2^+,[28,29] and Ar–HN_2^+.[30]

The strength of the Ne–HCO^+ intermolecular bond can be estimated from the perturbation expressions[25] for the intermolecular stretching frequency

$$\nu_s = \sqrt{\frac{4B_{\text{complex}}^3}{D_{\text{complex}}}\left(1 - \frac{B_{\text{complex}}}{B_{\text{HCO}^+}}\right)} \tag{3}$$

and the harmonic force constant

$$k_s = 16\pi^2 \mu c^2 B_{\text{complex}}^3 (1 - B_{\text{complex}}/B_{\text{HCO}^+})/D_{\text{complex}}. \tag{4}$$

For the ground state of ^{20}Ne–HCO^+ ($B_{\text{HCO}^+} = 1.488$ cm^{-1})[10] this yields $\nu_s = 83.3 \pm 2.5$ cm^{-1} and $k_s = 4.84 \pm 0.30$ N/m (Table I). In the ν_1 excited state ($B_{\text{HCO}^+} = 1.476$ cm^{-1})[10] the intermolecular bond is stronger, with a larger force constant ($k_s = 5.32 \pm 0.36$ N/m) and intermolecular stretching frequency ($\nu_s = 87.4 \pm 3.0$ cm^{-1}).

Apart from altering the Ne–HCO^+ rotational constants, the principal effect of the Ne atom isotopic substitution is to slightly shift the vibrational origin, due to different zero point energies for the intermolecular vibrations with the HCO^+ core in the ground and ν_1 states. It is probably a fair approximation to neglect the change in the zero point energy for the intermolecular bending vibration, for in this case the isotopic substitution of the Ne atom has quite a tiny effect on the reduced mass. Considering only the zero-point-energy effect of the intermolecular stretching vibration, in the harmonic approximation the separation of the isotopomer ν_1 origins is given by

$$\Delta = \frac{1}{2}(\nu_s' - \nu_s'')\left(\sqrt{\frac{\mu_{20}}{\mu_{22}}} - 1\right), \tag{5}$$

where ν' and ν'' are the harmonic frequencies for the intermolecular stretch vibration of ^{20}Ne–HCO^+ in the ground and ν_1 states, and μ_{20} and μ_{22} are the stretching vibration reduced masses for ^{20}Ne–HCO^+ and ^{22}Ne–HCO^+. Inserting the harmonic frequencies from Table I, one finds that $\Delta = -0.06 \pm 0.05$ cm^{-1}, consistent with the observed shift (-0.106 cm^{-1}).

Significantly, in the Ne–HCO^+ ν_1 spectrum there is no evidence for the type of isolated upper state perturbations, which were found to afflict several rotational levels in the ν_1 manifold of He–HCO^+.[5] For the He containing complex the perturbations were tentatively ascribed to an accidental resonance between ν_1 and the combination of the intramolecular $\nu_2 + \nu_3$ vibration with quanta of intermolecular modes ($\nu_2 + \nu_3 \approx 3012.3$ cm^{-1} in the free monomer[12]). In Ne–HCO^+ the ν_1 vibration is depressed by roughly 30 cm^{-1} compared to He–HCO^+, and it is possible that the interacting states have moved away from resonance. Further support for this hypothesis arises from the apparent absence of perturbations for the Ar–HCO^+ ν_1 band where the decrease in the ν_1 frequency is even more substantial.[6]

2. Radial one-dimensional Ne···HCO$^+$ potential

In order to estimate the dissociation energy and spacings for the higher intermolecular stretching states it is desirable to construct a radial Ne···HCO^+ potential energy function out to the dissociation limit. In the present work, the potential in the mid-range bonding region is obtained by employing the rotational Rydberg–Klein–Rees (RKR) procedure,[31,32] using the empirically obtained spectroscopic constants (B, D, and H values) as input. The long-range part of the potential is assumed to have the form appropriate for the classical polarization interaction between the Ne atom and a set of multipoles (charge, dipole, quadrupole, etc.) sited on the HCO^+ nuclei (with the multipoles being determined from *ab initio* calculations). This approach has been previously applied to the related ionic He–HN_2^+ complex, and the reader is directed to Ref. 4 for more details.

The rotational RKR inversion method relies on the Bohr quantization condition for the phase integral, where the integration limits are the classical turning points of the potential. By assuming a harmonic potential and expressing the energy $E(v,J)$ as a power series in $(v+1/2)$ and $J(J+1)$, it is possible to solve the RKR integrals analytically and extract

TABLE II. Atom-centered spherical tensor multipole moments for the linear HCO^+ molecule obtained from *ab initio* calculations described in the text. Q_0, Q_1, and Q_2 are the charge, dipole, and quadrupole moments.

	H	C	O
Q_0/e	0.371	0.561	0.068
Q_1/ea_0	0.164	−0.278	−0.092
Q_2/ea_0^2	0.20	−0.753	−0.086

the turning points. These points are subsequently fitted to an anharmonic model potential $V(r)$, the exact form of which is not crucial for the results.[31] Employing this fitted reference potential, more accurate anharmonic expressions for the vibrational dependence of $E(v,J)$ and $B(v,J)$ are obtained. With these, an improved set of turning points are determined which are again fitted by a reference potential. This process is repeated until convergence is achieved. Explicit expressions for the turning points in terms of the derivatives of the reference potential and the experimentally determined rotational constants are given in Refs. 31 and 32. In this case, the reference potential function consists of an expansion in $(r-r_e)/r$ terminated at the cubic term:

$$V(r)=a+b\left(\frac{r-r_e}{r}\right)^2+c\left(\frac{r-r_e}{r}\right)^3. \tag{6}$$

After a few iterations of the procedure the residuals of the RKR points to the fitted function were less than 0.1 cm^{-1}. The experimental data ($v_1=0$ and 1, $J=0-60$) provide RKR turning points of the intermolecular potential in the region between 3.48 and 3.90 Å. Inclusion of H values did not influence the potential significantly, i.e., the energy levels and center-of-mass distances were the same within 2 cm^{-1} and 0.002 Å.

The mid-range RKR potential is extended to longer ranges by considering the classical polarization energy for the Ne···HCO^+ interaction. This part of the potential is approximated by the induction interaction between the Ne atom and a set of multipoles distributed over the HCO^+ molecule which are determined using the CADPAC program package[33] (distributed multipole analysis, DMA[34]). The basis functions employed in the calculation consist of a triple zeta basis set, augmented by two diffuse and one polarization function on each center: on the O atom $(10s,5p,2d,1f)\rightarrow[4s,3p,2d,1f]$ plus two s functions with exponents of 0.08 and 0.025 and an f function with exponent 1; on the C atom $(10s,5p,2d,1f)\rightarrow[4s,3p,2d,1f]$ plus two s functions with exponents of 0.04 and 0.01 and an f function with exponent 1; and on the H atom $(5s,2p,1d)\rightarrow[3s,2p,1d]$ plus two diffuse s and one d function with exponents 0.05, 0.015, and 1.0, respectively. The distributed spherical tensor multipoles (up to quadrupole) calculated from the experimentally determined equilibrium distances ($r_{OC}=1.1096$ Å, $r_{CH}=1.0964$ Å)[15] are listed in Table II.

TABLE III. Parameters for the one-dimensional radial potentials for Ne interacting with HCO^+ in its ground (000) and the ν_1 excited (100) states [Eqs. (6) and (7), see also Fig. 2]. r_j and w are parameters of the switching functions defined in Ref. 4.

	Ne···HCO^+ (000)	Ne···HCO^+ (100)
r_j	3.913	3.885
w	10	10
a (cm^{-1})	−44.65	−48.23
b (cm^{-1})	1.882×10^4	2.181×10^4
c (cm^{-1})	-2.592×10^4	-2.793×10^4
r_e (Å)	3.644	3.637
c_0 (cm^{-1})	4.18×10^2	4.33×10^2
c_4 (cm^{-1} Å^4)	-4.65×10^4	-4.65×10^4
c_6 (cm^{-1} Å^6)	2.09×10^5	2.09×10^5
c_8 (cm^{-1} Å^8)	-1.328×10^7	-1.328×10^7

The induction potential arising from the interaction of the multipoles with the Ne atom ($\alpha=0.3960$ Å^3) is fitted for $\theta=0$ to the following function:

$$V_{\mathrm{ind}}(r)=c_0+\sum_{n=2}^{4}\frac{c_{2n}}{r^{2n}}, \tag{7}$$

where r is the distance between the Ne atom and the HCO^+ center-of-mass. Finally, the long-range polarization potential is smoothly connected to the mid-range RKR potential at the outermost turning point (r_j) using the appropriate offset parameter c_0 and switching functions (described in Ref. 4). Complete sets of parameters for the intermolecular potentials obtained for the (000) and (100) states are listed in Table III.

In order to calculate the energies of the intermolecular vibrational stretching levels, the one-dimensional Schrödinger equation was solved numerically for the potentials derived for Ne interacting with HCO^+ in its (000) and (100) states.[35] The resulting frequencies for the first seven intermolecular vibrational states are compiled in Table IV along with the respective dissociation energies (D_0 and D_e). Figure 2 illustrates the Ne···HCO^+(000) potential, along with the intermolecular stretch vibrational energy levels.

TABLE IV. Data for the one-dimensional Ne···HCO^+ radial potentials (Fig. 2). Included are energies for the lowest seven vibrational levels $E(v)$, dissociation energies (D_0 and D_e), and center-of-mass equilibrium distances (r_e).

HCO^+ vibrational state	D_0 (cm^{-1})	D_e (cm^{-1})	r_e (Å)	$E(1)$ (cm^{-1})	$E(2)$ (cm^{-1})	$E(3)$ (cm^{-1})	$E(4)$ (cm^{-1})	$E(5)$ (cm^{-1})	$E(6)$ (cm^{-1})	$E(7)$ (cm^{-1})
(000)	438.08	483.13	3.644	86.8	165.3	228.0	278.4	317.7	347.8	370.3
(100)	454.12	502.37	3.637	93.3	175.6	240.2	291.9	332.1	362.7	385.4

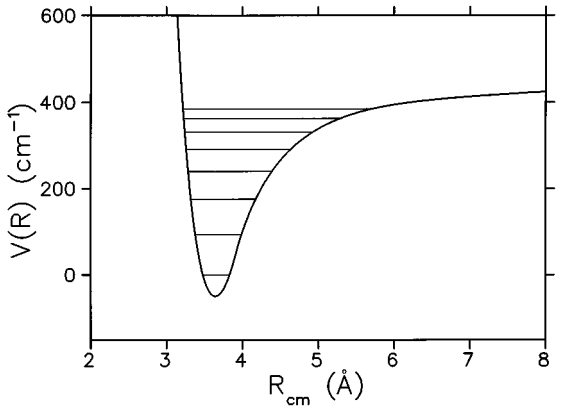

FIG. 2. One-dimensional radial intermolecular potential, along with the first seven vibrational levels for the collinear interaction of Ne and HCO^+ in its vibrationless state. The mid-range part of the potential (between 3.48 and 3.90 Å) is obtained by the RKR procedure using the spectroscopic rotational constants of ^{20}Ne–HCO^+ (Table I). The long-range part of the potential is constructed by joining the RKR potential to the polarization interaction potential obtained from the distributed multipole analysis.

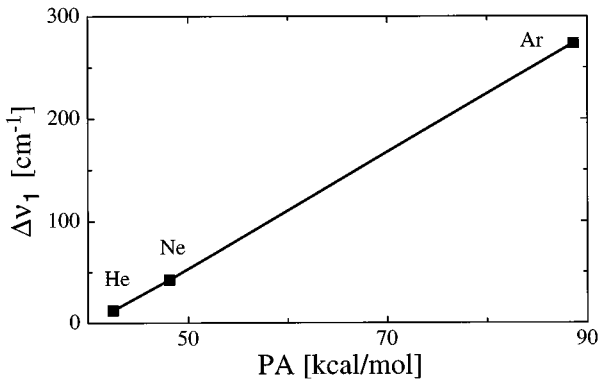

FIG. 3. Complexation induced ν_1 redshifts for a variety of Rg–HCO^+ complexes as a function of the proton affinity (PA) of the rare gas (Rg=He, Ne, and Ar).

3. Discussion

The spectroscopic data and the rotational RKR/DMA potentials demonstrate that Ne–HCO^+ is a relatively strongly bound complex ($D_0'' \approx 438$ cm^{-1}), possessing a linear proton-bound structure, a center-of-mass intermolecular separation of roughly 3.65 Å, and an estimated intermolecular stretching frequency of 87 cm^{-1}. The intermolecular interaction between the Ne atom and the HCO^+ core becomes slightly more attractive upon ν_1 excitation as evidenced by the shorter intermolecular bond and the larger intermolecular stretch frequency (Tables I and IV). The complexation induced redshift of the HCO^+ ν_1 frequency (42.5 cm^{-1}) is also a symptom of a stronger Ne$\cdots$$HCO^+$ bond in the (100) state.

Although solution of the radial Schrödinger equation using the RKR/DMA potential yields an intermolecular stretching frequency of roughly 90 cm^{-1}, there is no evidence for a band displaced by this amount from ν_1 in the Ne–HCO^+ mid-infrared spectrum. There is however, some rather weak activity in both the Ne–HCO^+ and the Ne_2–HCO^+ spectra around 67 cm^{-1} above the ν_1 origin, although this could also be either $\nu_1+\nu_b$ (ν_b is the intermolecular bend) or $\nu_2+\nu_3$.

The present study puts us in a position to compare the properties of Ne–HCO^+ with other rare gas containing proton-bound complexes (Rg–HCO^+, Rg=He and Ar) as well as with the related isoelectronic neutral van der Waals complexes of the type Rg–HCN (Rg=He, Ne, and Ar). Considering the ions first, we note that as expected, the strength of the intermolecular bond in the HCO^+ containing species increases in the order He<Ne<Ar, in line with proton affinities and polarizabilities of the attached bases. Thus, the radial force constants for He–HCO^+, Ne–HCO^+, and Ar–HCO^+ are 1.64,[5] 4.84, and ≈21 N/m.[6] The ν_1 redshifts, which reflect the influence of the rare gas on the effective proton potential, vary in the same way: 12.5, 42.5, and 246.5 cm^{-1} for the He, Ne, and Ar containing complexes, respectively. Interestingly, the average intermolecular separation does not depend strongly upon the rare gas atom: in He–HCO^+ (3.66 Å) it is almost the same as in Ne–HCO^+ (3.65 Å) and Ar–HCO^+ (3.80 Å). The similarity is most probably due to a cancellation of competing effects; while the polarization attraction is stronger for larger rare gas atoms, their electron clouds are more extensive and overlap repulsion becomes important at longer intermolecular distances.

It would be interesting to ascertain the degree of proton transfer attending formation of the Ne–HCO^+ complex. Unfortunately, the rotational constants are rather insensitive to the position of the proton and their errors are too large to obtain any useful information in this regard. Nevertheless, an indirect indication of proton delocalization toward the rare gas is provided by the decrease in the HCO^+ ν_1 frequency, which presumably arises from a flattening of the effective proton potential under the influence of the second center of attraction. The ν_1 redshift can again be correlated with the proton affinity of the added base (see Fig. 3). In extreme cases, where two identical bases are bound to one another, calculations show that the frequency can drop by more than 50% (He–H–He^+).[36]

There appear to be essential differences between ionic complexes of the form Rg–HCO^+ and their isoelectronic neutral counterparts Rg–HCN. Although both ions and neutrals share a common linear minimum energy geometry, with the proton occupying an intermediate position, the ions are considerably more strongly bound and feature a somewhat stiffer intermolecular bending coordinate. For example, while the combined RKR/DMA potential for Ne–HCO^+ has a D_0 value of 438 cm^{-1}, the binding energy[8] for Ne–HCN is only 37 cm^{-1}. Interestingly, the force constant for the Ne$\cdots$$HCO^+$ bond is of the same order as it is in weakly hydrogen-bonded systems (e.g., H_2O–HCCH k_s=6.5 N/m).[37] Differences between neutrals and ions extend also to the complexation induced redshifts in ν_1. Although there do not appear to be any mid-IR data for the Ne–HCN van der Waals molecule, the redshift is expected to be less than it is for Ar–HCN (2.69 cm^{-1}).[38]

Unfortunately, the present study provides little information on the angular characteristics of the Ne$\cdots$$HCO^+$ inter-

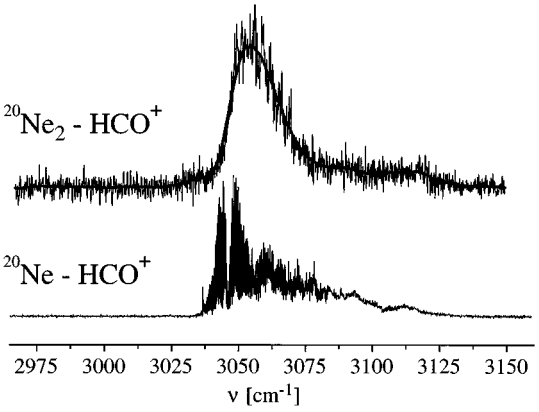

FIG. 4. Comparison of the vibrational photodissociation spectra of $^{20}Ne_2$–HCO^+ and ^{20}Ne–HCO^+ in the ν_1 region (C–H stretch). In both cases the spectra are obtained by monitoring the HCO^+ fragment current as a function of photon frequency.

molecular bond. In the related He–HN_2^+ complex the $\nu_1+\nu_b$ combination band (C–H stretch plus intermolecular bend) has been observed 96 cm^{-1} above ν_1, suggesting a pronounced preference for a linear structure and it does not seem unreasonable to assume that Ne–HCO^+ also possesses a comparatively stiff intermolecular bending coordinate. For isoelectronic, neutral ball-and-stick van der Waals molecules the intermolecular bending motion can be extremely floppy resulting in extreme stretch-bend interactions. The most thoroughly analyzed example is Ar–HCN, which features a large centrifugal distortion constant that arises not so much because of facile radial bond deformation, but is rather a consequence of an extremely large zero-point bending amplitude, coupled with a potential surface where the radial equilibrium separation diminishes substantially as the system moves away from its linear minimum.[39] It is perhaps significant to note that the D value for Ne–HCO^+ is around two orders of magnitude smaller than for Ne–HCN,[8] indicating that extreme angular-radial couplings are probably of less importance in the ion. Still, it may be prudent to regard the Ne–HCO^+ radial force constants and intermolecular stretching frequencies as provisional lower bounds.

B. Ne_2–HCO^+

The (100) band of the Ne_2–HCO^+ trimer was recorded by monitoring its photofragmentation into the HCO^+ monomer (see Fig. 4). No Ne–HCO^+ photofragment ions were detected, and given the S/N ratio for the measurements, we estimate that the branching ratio for the two possible photofragmentation channels $n=2\rightarrow n=0$ and $n=2\rightarrow n=1$ is at least 10. The spectrum of the trimer (Fig. 4) exhibits a single broad peak (full width at half-maximum $\approx$20 cm^{-1}) in marked contrast with the clearly rotationally resolved dimer spectrum. For reasonable trimer structures, given the 0.02 cm^{-1} laser bandwidth, the rotational constants should be large enough for the spectrum to be at least partially resolved. The corresponding Ar_2–HCO^+ (Ref. 6) and He_2–HN_2^+ (Ref. 4) trimers also exhibit broadened ν_1 bands. Possible reasons for the lack of resolved rotational features have been discussed in Ref. 6, and include homogeneous lifetime broadening due to rapid vibrational predissociation or energy redistribution, and the overlapping of vibrational sequence bands and bands due to different isomers.

Of some interest are the complexation-induced vibrational band shifts for Ne–HCO^+ and Ne_2–HCO^+. While the Ne–HCO^+ ν_1 band origin is appreciably redshifted from the monomer one (by 42.5 cm^{-1}), the addition of a second Ne atom shifts the transition slightly back to higher energy (by 8 ± 3 cm^{-1}). Again, this is in line with observations for the Ar_n–HCO^+ (Ref. 6) and He_n–HN_2^+ complexes.[4] The connection between structures and vibrational band shifts for rare-gas containing proton-bound complexes has been discussed in Ref. 6. In the larger clusters ($n>1$), a single rare-gas atom appears to occupy a linear proton-bound position, effectively forming a dimer core to which further rare-gas atoms are more loosely bonded in primary and secondary solvation rings (each containing four or five rare gases). It is the terminal, proton-bound rare-gas atom that is primarily responsible for the flattened effective proton potential and consequent decrease in the ν_1 frequency. The additional rare-gas atoms crowd about the proton, nudging the terminal rare-gas atom further away, thereby diminishing its flattening effect on the effective proton potential and leading to the small incremental blueshifts.

IV. CONCLUSIONS

The mid-infrared spectrum of Ne–HCO^+ (ν_1 C–H stretch band) confirms that in common with other similar previously characterized complexes, it possesses a linear proton-bound minimum energy structure. An estimate of 438 cm^{-1} for the dissociation energy (D_0) is obtained by combining a RKR potential developed using the experimental rotational constants, with the long-range polarization potential. Using the same potential the $(\nu_1+\nu_s)-\nu_1$ spacing is estimated to be 90 cm^{-1}. Laser limited rotational linewidths allow one to put a lower limit of approximately 250 ps on the lifetime of the upper state. A particular focus of future experimental work will be to obtain spectra of bands involving the intermolecular stretching and bending modes ($\nu_1+\nu_s$ and $\nu_1+\nu_b$) in order to provide more detailed information on the Ne$\cdots$$HCO^+$ intermolecular potential. The sensitivity of the IR predissociation approach is emphasized by the observation of the ^{22}Ne–HCO^+ spectrum with the complex being synthesized using ^{22}Ne in its natural abundance ($\approx$9%). The $^{20}Ne_2$–HCO^+ ν_1 band is blueshifted by 8 ± 3 cm^{-1} with respect to that of ^{20}Ne–HCO^+, consistent with a trimer structure where the second Ne atom is loosely attached to the linear Ne–HCO^+ dimer core.

ACKNOWLEDGMENTS

This study is part of Project No. 20-41768.94 of ''Schweizerischer Nationalfonds zur Förderung der wissenschaftlichen Forschung.'' Support through the Human Capi-

tal and Mobility program ''Structure and Reactivity of Molecular Ions'' (BBW Grant No. 93.02060) is gratefully acknowledged.

[1] M. Bogey, H. Bolvin, C. Demuynck, J. L. Destombes, and B. P. Van Eijck, J. Chem. Phys. **88**, 4120 (1988).
[2] Y. B. Cao, J. H. Choi, B. M. Haas, M. S. Johnson, and M. Okumura, J. Phys. Chem. **97**, 5215 (1993).
[3] S. A. Nizkorodov, J. P. Maier, and E. J. Bieske, J. Chem. Phys. **102**, 5570 (1995).
[4] M. Meuwly, S. A. Nizkorodov, J. P. Maier, and E. J. Bieske, J. Chem. Phys. **104**, 3876 (1996).
[5] S. A. Nizkorodov, J. P. Maier, and E. J. Bieske, J. Chem. Phys. **103**, 1297 (1995).
[6] S. A. Nizkorodov, O. Dopfer, T. Ruchti, M. Meuwly, J. P. Maier, and E. J. Bieske, J. Phys. Chem. **99**, 17118 (1995).
[7] E. J. Bieske, S. A. Nizkorodov, F. R. Bennett, and J. P. Maier, J. Chem. Phys. **102**, 5152 (1995).
[8] H. S. Gutowsky, J. D. Keen, T. C. Germann, T. Emilsson, J. D. Augspurger, and C. E. Dykstra, J. Chem. Phys. **98**, 6801 (1993).
[9] T. Amano, J. Chem. Phys. **79**, 3595 (1988).
[10] C. S. Gudeman and R. J. Saykally, Annu. Rev. Phys. Chem. **35**, 387 (1984).
[11] K. Kawaguchi, C. Yamada, S. Saito, and E. Hirota, J. Chem. Phys. **82**, 1750 (1985).
[12] D. J. Liu, S. T. Lee, and T. Oka, J. Mol. Spectrosc. **128**, 236 (1988).
[13] S. C. Foster, A. R. W. McKellar, and T. J. Sears, J. Chem. Phys. **81**, 578 (1984).
[14] K. V. L. N. Sastry, E. Herbst, and F. C. De Lucia, J. Chem. Phys. **75**, 4169 (1981).
[15] R. C. Woods, Philos. Trans. R. Soc. London Ser. A **324**, 141 (1988).
[16] A. Koch, M. C. van Hemert, and E. F. Disoeck, J. Chem. Phys. **103**, 7006 (1995); and references therein.
[17] N. G. Adams and D. Smith, Int. J. Mass Spectrom. Ion Phys. **21**, 349 (1976).
[18] S. G. Lias, J. E. Bartmess, J. F. Liebman, J. L. Holmes, R. D. Levin, and W. G. Mallard, J. Phys. Chem. Ref. Data **17**, (1988).
[19] N. R. Daly, Rev. Sci. Instrum. **31**, 264 (1960).
[20] E. J. Bieske, Faraday Trans. **91**, 1 (1995).
[21] M. J. McEwan, in *Advances in Gas Phase Ion Chemistry*, edited by N. G. Adams and L. M. Babcock (JAI, Connecticut, 1992).
[22] R. H. Nobes and L. Radom, Chem. Phys. **60**, 1 (1981).
[23] M. F. Jarrold, M. T. Bowers, D. J. DeFrees, A. D. McLean, and E. Herbst, Astrophys. J. **303**, 392 (1986).
[24] G. Guelachvili and K. N. Rao, *Handbook of Infrared Standards* (Academic, London, 1993), Vol. 2.
[25] D. J. Millen, Can. J. Chem. **63**, 1477 (1985).
[26] D. J. Nesbitt, Chem. Rev. **88**, 843 (1988).
[27] D. A. Dixon, A. Komornicki, and W. P. Kraemer, J. Chem. Phys. **81**, 3603 (1984).
[28] W. P. Kraemer, A. Komornicki, and D. A. Dixon, Chem. Phys. **105**, 87 (1986).
[29] E. J. Bieske, S. A. Nizkorodov, F. Bennett, and J. P. Maier, Int. J. Mass Spectrom. Ion Proc. **149/150**, 167 (1995).
[30] M. Kolbuszewski, Chem. Phys. Lett. **244**, 39 (1995).
[31] M. S. Child and D. J. Nesbitt, Chem. Phys. Lett. **149**, 404 (1988).
[32] D. J. Nesbitt, M. S. Child, and D. J. Clary, J. Chem. Phys. **90**, 4855 (1989).
[33] R. D. Amos, I. L. Alberts, J. S. Andrews, S. M. Colwell, N. C. Handy, D. Jayatilaka, P. J. Knowles, R. Kobayashi, N. Koga, K. E. Laidig, P. E. Maslen, C. W. Murray, J. E. Rice, J. Sanz, E. D. Simandiras, A. J. Stone, and M-D. Su, *The Cambridge Analytical Derivatives Package* (Cambridge University Press, Cambridge, 1992), Issue No. 5.
[34] A. J. Stone, Chem. Phys. Lett. **83**, 233 (1981).
[35] R. J. Le Roy, University of Waterloo, Chemical Physics Report No. CP-330 Level 5.0, 1991.
[36] J. S. Lee and D. Secrest, J. Chem. Phys. **85**, 6565 (1986).
[37] K. I. Peterson and W. Klemperer, J. Chem. Phys. **81**, 3842 (1984).
[38] G. T. Fraser and A. S. Pine, J. Chem. Phys. **91**, 3319 (1989).
[39] S. Drucker, A. L. Cooksy, and W. Klemperer, J. Chem. Phys. **98**, 5158 (1993).